NASA/TM—2001-211113

Non-Intrusive, Laser-Based Imaging of Jet-A Fuel Injection and Combustion Species in High Pressure, Subsonic Flows

Randy J. Locke
QSS Group, Inc., Brook Park, Ohio

Yolanda R. Hicks and Robert C. Anderson
Glenn Research Center, Cleveland, Ohio

Wilhelmus A. de Groot
QSS Group, Inc., Brook Park, Ohio

Prepared for the Joint
First Modeling and Simulation Subcommittee Meeting,
25th Airbreathing Propulsion Subcommittee Meeting,
37th Combustion Subcommittee Meeting, and the
19th Propulsion Systems Hazards Subcommittee Meeting
sponsored by the Joint Army-Navy-NASA-Air Force
Monterey, California, November 13–17, 2000

National Aeronautics and
Space Administration

Glenn Research Center

August 2001

Acknowledgments

The authors would like to acknowledge the contributions of Dr. Changlie Wey, Dr. Quang-Viet Nguyen, and Dr. Dan Bulzan of the NASA Glenn Combustion Branch for making the proprietary injector available for this study.

This report is a formal draft or working paper, intended to solicit comments and ideas from a technical peer group.

This report contains preliminary findings, subject to revision as analysis proceeds.

Available from

NASA Center for Aerospace Information
7121 Standard Drive
Hanover, MD 21076

National Technical Information Service
5285 Port Royal Road
Springfield, VA 22100

Available electronically at http://gltrs.grc.nasa.gov/GLTRS

Non-Intrusive, Laser-Based Imaging of Jet-A Fuel Injection and Combustion Species in High Pressure, Subsonic Flows

Randy J. Locke
QSS Group, Inc.
Brook Park, Ohio 44142

Yolanda R. Hicks and Robert C. Anderson
National Aeronautics and Space Administration
Glenn Research Center
Cleveland, Ohio 44135

Wilhelmus A. de Groot
QSS Group, Inc.
Brook Park, Ohio 44142

ABSTRACT

The emphasis of combustion research efforts at NASA Glenn Research Center (GRC) is on collaborating with industry to design and test gas-turbine combustors and subcomponents for both sub- and supersonic applications. These next-generation aircraft combustors are required to meet strict international environmental restrictions limiting emissions. To meet these goals, innovative combustor concepts require operation at temperatures and pressures far exceeding those of current designs. New and innovative diagnostic tools are necessary to characterize these flow streams since existing methods are inadequate. The combustion diagnostics team at GRC has implemented a suite of highly sensitive, nonintrusive optical imaging methods to diagnose the flowfields of these new engine concepts. By using optically accessible combustors and flametubes, imaging of fuel and intermediate combustion species via planar laser-induced fluorescence (PLIF) at realistic pressures are now possible. Direct imaging of the fuel injection process through both planar Mie scattering and PLIF methods is also performed. Additionally, a novel combination of planar fuel fluorescence imaging and computational analysis allows a 3-D examination of the flowfield, resulting in spatially and temporally resolved fuel/air volume distribution maps. These maps provide detailed insight into the fuel injection process at actual conditions, thereby greatly enhancing the evaluation of fuel injector performance and other combustion phenomena. Stable species such as CO_2, O_2, N_2, H_2O, and hydrocarbons are also investigated by a newly demonstrated 1-D, spontaneous Raman spectroscopic method. This visible wavelength Raman technique allows the acquisition of quantitative, stable species concentration measurements from the flow.

INTRODUCTION

The next generation of gas turbine aircraft combustors will be required to meet stringent environmental restrictions mandating a 50% – 75% reduction in NO_x emissions over existing levels. In order to meet emission reduction goals, future power plant concepts will incorporate operational conditions far exceeding those of current designs[1]. At these conditions of extreme pressure and temperature, innovative diagnostic tools will be required to obtain the desired measurements since existing methods are inadequate. Additionally, these measurements need to be more quantitative as well as spatially and temporally resolved in order to understand more fully the physical processes leading to the formation of undesired emissions. Furthermore, the measurements as well as the analyses need to be quicker to provide more immediate combustor and combustor subcomponent performance feedback to designers.

Our efforts at the engine research facilities at NASA Glenn Research Center embrace a partnership with industry to design and develop aeropropulsion gas turbine combustors and subcomponents to meet or exceed these new international emissions reduction requirements. To that end, the advanced combustion diagnostics team at GRC has designed several large-scale, high pressure and high temperature, optically accessible, sector combustor and flametube test sections. These test sections allow the implementation of a wide array of optical techniques to non-intrusively probe the fuel-air mixing processes and other flowfield phenomena of these concept combustors. High pressure reacting flowfields burning jet fuel are now routinely imaged within GRC propulsion research laboratories where ten years ago, imaging of the planar laser-induced fluorescence (PLIF) from species within an actual combustor was thought beyond reach due to the limitations imposed by pressure-induced quenching of the excited state.

In the ten years since the advanced diagnostic effort at NASA Glenn was implemented, we have made many advances in the application of a wide variety of nonintrusive, optical, and mostly imaging techniques in the harsh environment of high pressure, liquid-fueled, gas turbine combustors. PLIF imaging of jet fuel, NO, and intermediate flame species such as OH, at pressures approaching 20 atms have been reported previously[2] and are now routinely performed in analyzing combustor subcomponent performance characteristics. Imaging of the fuel injection process, or spray patternation, by both PLIF and planar Mie scattering is also now routinely performed[3] to aid fuel injector designers who, until recently, have been unable to directly view in real-time the fuel injection process under realistic conditions. Phase Doppler particle anemometry (PDPA) has also been applied to the non-reacting and reacting flowfields[3] to obtain the first ever quantitative droplet size and velocity measurements from these liquid-fueled flowfields. A comparison of PLIF and planar Mie scattering imaging (PMie) with simultaneous PDPA has also provided a means to quantify previously qualitative data.

Other recent efforts have also demonstrated[4] that it is feasible to obtain one-dimensional quantitative major species concentration data in a gas turbine engine using a tunable, excimer laser operating at UV wavelengths. With a careful selection of laser wavelength it was possible to obtain major species 1-D images and spectra without substantial LIF interference. It was found that the main advantage of using UV light for spontaneous Raman was the enhanced signal strength ($\propto 1/\lambda^4$), which could make single shot (time resolved) quantitative Raman feasible.

EXPERIMENTAL

The experimental apparatus for the measurements reported herein are described in detail elsewhere.[5] For the PLIF measurements the optical set-up and test rig comprise a 10 Hz doubled dye Nd:YAG laser and high pressure flametube. The doubled dye output at approximately 281.5 nm, is directed 18 meters through an enclosed dual-beam, optical path to the test rig, as shown in figure (1). The dual-beam path allows the use of two Nd:YAG systems for simultaneous, and/or two-color experiments.

The optically accessible flametube has four mutually perpendicular, film-cooled, UV-grade, fused silica windows, measuring 2.5 inches axially, 1.5 inches radially, and 0.5 inch thick. This design allows views of approximately 67% of the entire flowfield. A schematic of this experimental setup is shown in figure (2). For planar measurements, shown in Figure 2 (left), the nominally 15 mJ, 283 nm laser beam is expanded into a sheet by a 3000 mm focal length, cylindrical lens and then passed through the top window of the test section. A gated and intensified CCD camera, fitted with a remotely controlled filter wheel containing up to five different 50 mm-diameter filters, collects the scattered laser light or fluorescence from prepared molecular species. The filter wheel allows the use of the same optical path for the acquisition of each data set. This allows direct comparison of images of multiple molecular species or flow phenomena with the same laser simply by changing the filter.

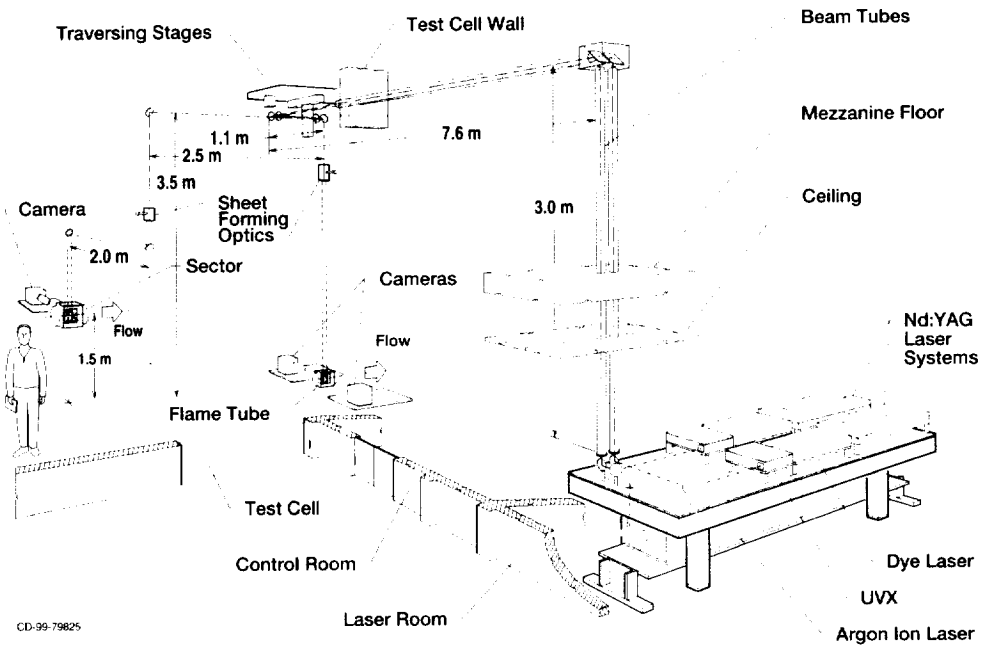

Figure 1. Experimental layout for performing optical diagnostics in high pressure gas turbine combustion.

Due to the physical restrictions imposed by the hardware and the extreme conditions of the flowfield it is impossible to obtain direct images of the cross-flow view looking upstream into the fuel injector. Since this view is desirable, a post data processing method was developed for extracting 3-dimensional flowfield information. This method combines a number (41 for this work) of sideview images taken at 1mm increments across the laser insertion window creating an image block. This image block can then be sliced to obtain views of the flow from any perspective interpolating between pixels where necessary.

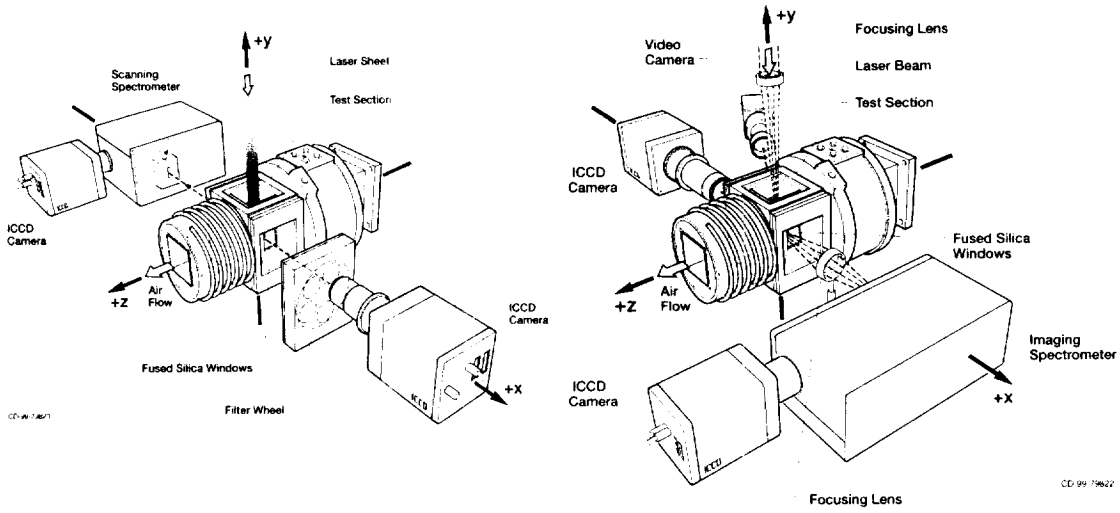

Figure 2. (Left) Close-up schematic detailing the planar data acquisition system and optically accessible test section. The flow is from right to left with the laser sheet entering from the top. (Right) Schematic of the optically accessible test section setup for visible wavelength Raman.

The beam delivery optics and collection scheme for the visible (λ=532 nm) spontaneous Raman imaging system are shown in Figure 2 (right). A 50 mm diameter, 400 mm focal length lens mounted above the flametube focuses the linearly polarized laser beam down into the test area. The laser beam polarization vector is parallel to the flametube flow direction. A 50 mm diameter, 200 mm focal length lens collects the scattered light at a 90° angle from the incident beam and perpendicular to the flow direction. In the absence of a Raman notch filter, a 550 nm high pass filter is placed in the collimated light collected by the collection lens. A 50 mm diameter, 100 mm focal length lens focuses the collected light into a 0.3 m spectrometer. A 300-groove/mm grating provides a 140 nm spectral range, sufficient to obtain simultaneous spectra of all major combustion species. A 384 x 576 pixel ICCD camera, with the 576 pixels in wavelength direction is mounted on the exit plane of the spectrometer. A calibration based on a multiple slit-equipped ruler, backlit through the slits, shows that an 18.3 mm section of the laser beam is imaged on the 384 pixel vertical CCD axis, or 48 μm per pixel. Downstream resolution was approximately 200 μm per pixel, set by the 100 μm spectrometer entrance slit. Laser pulse energy averaged 50 mJ/pulse, but because the imaged width of the laser beam was larger than the entrance slit, not all energy was utilized for imaging purposes.

RESULTS AND DISCUSSION

PLANAR IMAGING

A benefit of using the same optical path for all data acquisition is to be able to directly compare optical measurements without having to correct for different cameras or different optical paths. Figure (3) presents such a comparison of 50 laser-shot averaged cross-flow images obtained from a hollow cone injector operating at conditions of 5.3 atm pressure, 520K inlet air and equivalence ratio (ϕ) = 0.288. The figure displays the images at the indicated distance in millimeters from the fuel injector exit plane. The images were obtained at the identical conditions during the same test using the remotely controlled filter wheel previously described. Low temperature flow conditions were used for this examination to allow observation of Mie scattering from liquid fuel since at higher temperatures the fuel was completely vaporized.

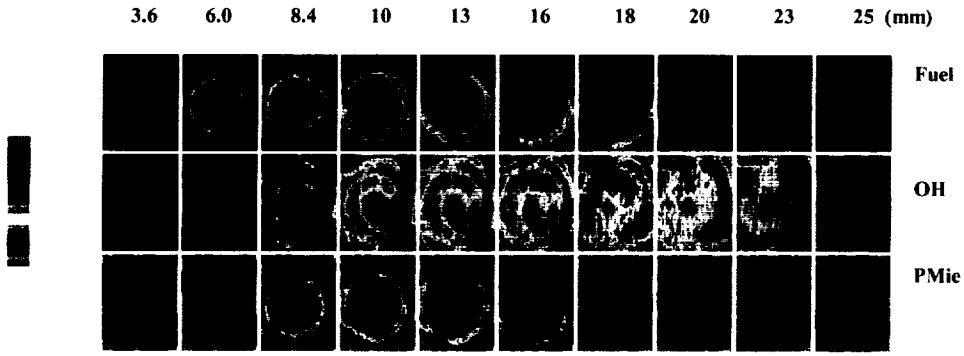

Figure 3. A comparison of cross-flow view images acquired for a hollow cone injector burning Jet-A fuel. Fuel PLIF, excited at λ = 281.5 nm (top), OH PLIF excited with the R_1(10) line at λ= 281.517 nm (middle), and planar Mie scattering elicited at 281.5 nm. The distance from the injector increases from left to right

Fuel PLIF images (top) were acquired by exciting the flowfield at 281.5 nm and collected by using a 2.6 nm FWHM, narrowband interference filter centered at 338 nm. The background corrected OH images (middle) were acquired by exciting the OH R_1(10) line at 281.517 nm and collected using a 1.6 nm FWHM narrowband interference filter centered at 316 nm. The OH background correction images were acquired by exciting off-line at 281.5 nm and collected using the same 1.6 nm FWHM filter. Mie scattering images (bottom) were acquired by scattering the 281.5 nm laser sheet and collected by using a 2.6 nm FWHM narrowband filter centered at 283 nm. Fuel PLIF and PMie images were corrected for background by subtracting an image acquired without laser excitation.

The three sets of images are shown beginning at 3.6 mm from the injector exit plane on the left and ending with the rightmost image 25 mm downstream of the injector exit plane. In both the fuel PLIF and the Mie scattering image series, a well-defined ring of fuel fluorescence and scattered light respectively, is observed to expand as the view plane moves downstream. Fluorescence from both vapor and liquid jet fuel is observed in this series of images since both phases are present at the window location under these test conditions, while only scattering from liquid fuel droplets is observed in the Mie series.

In addition to expanding, both the Mie scattering and fuel fluorescence are observed to decrease in intensity as the view plane moves downstream from the injector exit plane. This decrease in observed intensity is due to the consumption of the fuel during the combustion process. The OH sequence of images displays two ring-like structures arising from the fluorescence of excited OH generated within the combustion zone. The dark band between the two bright bands corresponds with the location of the fuel ring in the fuel PLIF series. The OH image series also clearly shows that the OH rings expand as they travel farther from the injector. In fact, the outer structure grows out of the field of view leaving only the inner fluorescing component of OH, which by the last image in the sequence has almost filled the entire cone. Also, in stark contrast to the fuel and Mie images, the OH fluorescence intensity is observed to increase with increasing distance from the injector with the exception of the last image. This apparent fall-off in the observed OH intensity in the final image in the series is attributable to two causes; first, the outer, stronger OH region has grown beyond the detector window dimensions and is lost to our field-of-view leaving only the central region of OH. The second cause is directly linked to our inability at the time to correct the images for non-homogeneities in the energy distribution across the excitation laser sheet. This is also a contributing factor in the PMie scattering and fuel fluorescence intensity drop-off. We have since instituted a correction process that will potentially allow us to show actual intensity trends in future tests.

Figure (4) presents a comparison between background corrected sideview fuel and OH PLIF images among those used to generate the cross-flow views seen in Figure (3). These images were acquired by imaging the fluorescence elicited when the excitation laser sheet was inserted into the flow at the hollow cone spray injector's centerline. The flow is from left to right. The left image shows the fuel PLIF obtained by exciting at 281.5 nm and detected using a 2.6 nm wide narrowband filter centered at 338 nm. The right image shows the OH PLIF obtained by exciting the OH, $R_1(10)$ line at 281.517 nm and detected using a 1.6 nm narrowband filter centered at 316 nm. The boundary of the region containing the top 80% of the total fuel PLIF signal from the left hand image, is shown by dashed lines in the OH image on the right. As can be seen, there is little OH fluorescence within these regions in the right-hand image. This signifies the presence of fuel and absence of reaction at these locations. There is however, a significant amount of OH signal observed both within and outside of the fuel spray cone outlined by the dashed lines, a feature not observed in the fuel PLIF image indicating that this diagnostic is an excellent method for showing physical characteristics of the fuel spray and location of the flame front.

Fuel PLIF OH PLIF with fuel traced

Figure 4: A Comparison of sideview images obtained from a hollow cone spray injector. Fuel PLIF (left) excited at 281.5, on-line OH PLIF (right), excited at 281.517 nm. The position of the region spanning the top 80% of the total fuel PLIF signal is outlined on the OH image.

In a series of experiments conducted for the purpose of evaluating the distribution of fuel injected into the flow stream, these imaging techniques and post-processing routines were used to generate fuel/air ratio contour maps. To illustrate, from the series of 41 sideview images, the fuel PLIF image taken at the centerline of a multi-point injector of proprietary design is shown in figure (5). For this investigation, the injector operated at conditions of: 755K inlet air temperature, 17 atm combustor pressure, f/a = 0.030 (Φ=0.44), 1.049 lb/sec of air mass flow, and 0.029 lb/sec of fuel mass flow. The fuel was injected radially into the main airflow at four, symmetrically arranged injection points. The injector exit plane is indicated in the figure by an arrow. With this injector, the fuel and air mixing region immediately downstream of the fuel injector was completely within view of the detector and laser sheet insertion windows. Additionally, the flamefront was stabilized well downstream of the window location, with the consequence that only fuel was present at the window location. These very specific conditions permitted the calibration of the data for fuel-to-air ratioing. The fuel was excited by a laser wavelength of 281.5 nm. The approximately 30 mm wide laser sheet entered the test section from above as indicated. The elicited fluorescence was detected by the filter wheel/ICCD assembly located perpendicular to the flow and incident laser sheet. In the figure, vertical lines indicate the locations and distances from the fuel injector exit plane at which cross-flow images were generated.

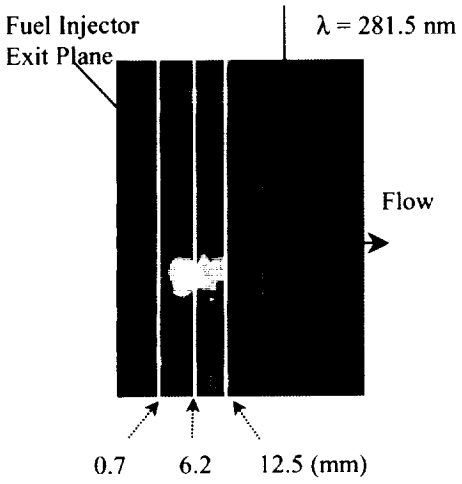

Figure 5. Sideview fuel PLIF image acquired from a flametube. Flow is from left to right. The Laser sheet, λ = 281.5 nm, travels from top to bottom. Conditions are T_{inlet} = 755K, $P_{combustor}$ = 17 atm, f/a = 0.030, w_{air} = 1.049 lbm/sec, w_{fuel} = 0,029 lb/sec.

As mentioned above, several conditions had to be met in this series of tests in order to generate fuel to air ratio (f/a) contour plots: a) the entire fuel injection cone is within the field of view over the width of the camera window; b) the premixed fuel is completely vaporized prior to reaching the window location; and c) the flame front is stabilized well downstream of the window position ensuring that no mechanism reduces the fuel concentration. These conditions were met by this injector and allowed us to make the assumption that the total amount of fuel remained constant across the field of view of the window for each of the six test conditions where only the equivalence ratio was varied. It was further assumed that all the fuel passing through the injector was available for excitation, fluorescence, and imaging. In this experiment, very little spreading of the injected fuel was observed over the downstream range of the windows. As a result, a cylinder could be carved from the generated data block encompassing all significant fuel fluorescence. The diameter of this cylinder was 20% larger than the injector exit and it's center was the injector centerline. For each of the six conditions tested, the average pixel value for the 3-D cylindrical image block was computed. The average values were then plotted against the global or total combustor fuel/air ratio and mapped to a straight line using a least squares criterion. This resulted in an expression for fuel/air ratio as a function of pixel value. Using this expression, the pixel values of the 3-D image blocks for each condition were then mapped to the global fuel/air ratio thereby creating 3-D, fuel/air ratio data blocks. The fuel/air ratio blocks can be oriented and sliced to produce cross-flow fuel/air ratio contour plots in the same fashion as the 3-D image blocks are sliced to produce PLIF or PMie cross-flow images.

The cross-flow fuel PLIF images (top row) and the resultant f/a contour plots (bottom) generated in the manner just described are presented in figure (6) for the f/a=0.030 test condition. In the left-most image of the fuel PLIF sequence, the four tightly drawn concentrics represent the areas of highest fuel concentration. These regions are symmetrically placed and correspond to the positions of the individual fuel injectors in this injector's design. As the distance from the injector exit plane increases (center and right images), a decrease in the fluorescence intensity, accompanied by a broadening and merging of the stronger intensity regions is observed. This is directly attributable to the effects of the mixing process. An increase in overall size of the fluorescent region is also observed, amounting to approximately 10% and stems from the divergence of the fuel spray as it moves downstream.

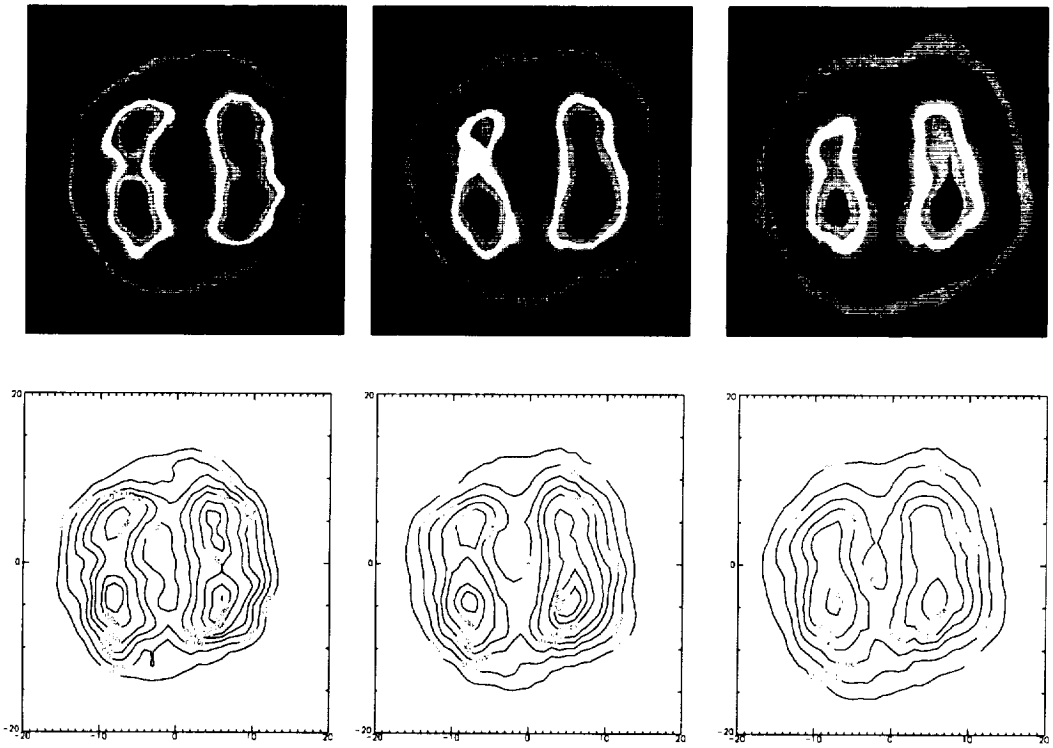

0.7 mm 6.2 mm 12.5 mm

Figure 6. A comparison of fuel PLIF cross-flow views (top) and fuel to air ratio contour plots (bottom) obtained at positions 0.7mm, 6.2mm, and 12.5mm downstream of the fuel injector denoted in figure 5. Flow conditions: T_{inlet}= 755K, P_{inlet}=17 atm, and ϕ= 0.44 (f/a= 0.030)

The fuel/air ratio contour maps generated for the same f/a = 0.030 test condition are presented in the bottom row in figure (6). The same features are found in these contour plots as were observed in the corresponding fuel PLIF cross-flow images. An approximate 10% increase in size of the fuel region, as well as a broadening and merging of the initially tight concentrics are both seen. Notable in these plots is a clearer indication of the presence of localized fuel rich regions. Contours with fuel/air maxima greater than 0.09 (ϕ=1.32) are observed in the left and middle plots. The regions of high fuel to air ratios in the left image merge and decrease markedly in value over the 5.5 mm to the location of the middle plot. In the right-hand plot, only six millimeters further downstream from the middle plot, all areas of high fuel/air values are gone, replaced by large regions of much lower f/a

values. Each of the other five test conditions examined during this series of experiments displayed similar results.

1-D, VISIBLE WAVELENGTH RAMAN

As previously stated, an earlier effort demonstrated that it was feasible to obtain one-dimensional quantitative major species concentration data in a gas turbine engine using a tunable excimer laser operating at UV wavelengths. The primary goal of the current effort was to reduce system cost and complexity by using one Nd:YAG laser system for spontaneous Raman imaging as well as for PLIF imaging. This required the use of the frequency-doubled line at 532 nm, and consequently a lower signal strength in comparison to the UV Raman. This lower signal strength was partially offset by the elimination of the PAH fluorescence in the visible wavelength Raman measurements. A comprehensive description of the advantages of UV or visible Raman techniques has been provided in the literature[6].

Figure (7a) and (7b) show a single-shot spectrum and a 100-shot averaged Raman spectrum obtained in air at 12 atm pressure and 480K inlet temperature, from an injector similar to that used to acquire the data shown in figures (5) and (6). Pixels in the horizontal direction image the Raman spectrum; pixels in the vertical direction image distance perpendicular to the flow axis. The strong vertical lines are the Raman images of oxygen and nitrogen. The narrow line widths are the result of the spectrometer slit width which provides good resolution but leads to loss in energy and signal to noise ratio (SNR). A horizontal streak is visible in the averaged image in figure (7b), indicating broadband emission, possibly caused by nitrogen plasma emission as the result of laser induced gas breakdown. A strong bright area is also visible on the shorter wavelength side of the oxygen line. This is likely light scattered into the spectrometer caused by insufficient shielding of the optics. A slant in the nitrogen and oxygen lines is also seen in the images, which indicates that the ICCD camera was not mounted square with respect to the spectrometer. The single-shot image in figure (7a) shows, although weak, both oxygen and nitrogen lines.

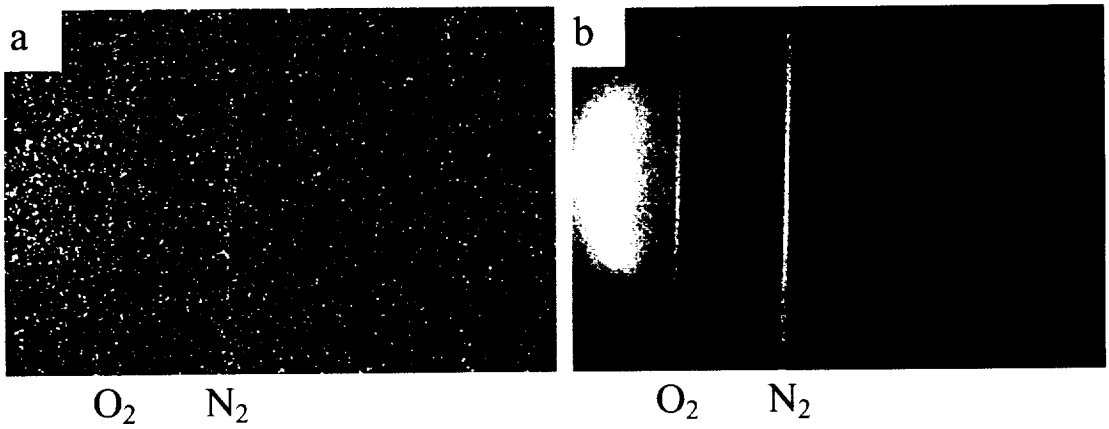

Figure 7: One-dimensional Raman images of nitrogen and oxygen at 480K and 12 atm; a. single-shot; b. 100-shot average

Figure (8) shows both a single-shot spectrum (a) and a 200-shot average spectrum (b) of air at 12 atm pressure and 480K inlet temperature. Again, the narrow line width is a result of the 100 μm spectrometer slit width. The SNR is lowest at the shorter wavelength portion of the spectrum, because laser line interference is strongest from Rayleigh, Mie, and surface reflections. Improved optics could substantially enhance the SNR. Such improvements include inserting a pinhole and better interference filters in the optics, as well as using more baffles and covers to reduce stray light interference. The averaged spectrum can be used to obtain optical collection efficiencies and relative species intensity relationships for quantitative measurements. However, the wide spectral range

covered in order to include all species reduces the resolution and accuracy available for quantitative measurements. Even though the laser output energy was 47 mJ per pulse, the actual energy used for spontaneous Raman measurement was substantially less due to delivery and collection optics losses, incurred to optimize spectral resolution.

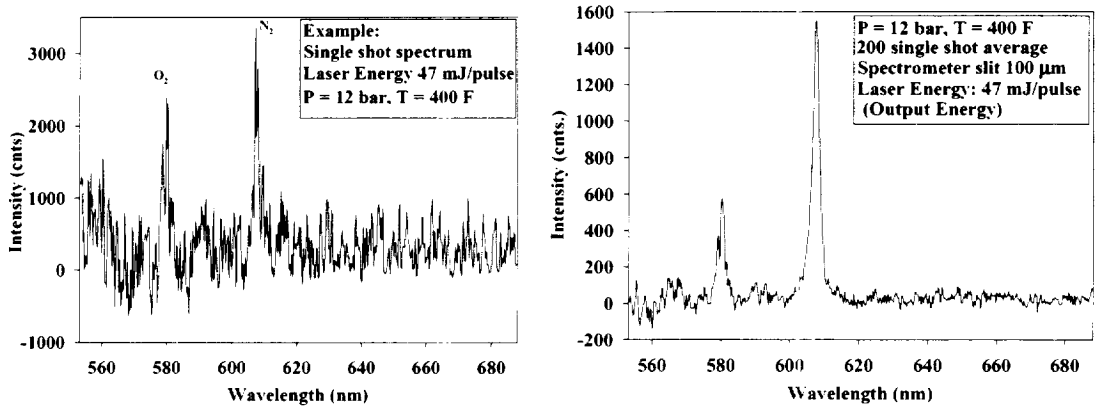

Figure 8: a: Single-shot spectrum and b: Averaged spectrum of high pressure air in combustor section

Raman measurements were also obtained with jet-A fuel injection into the combustor. Combustion takes place downstream of the measurement section, but fully or partially evaporated fuel mixes with air at the window location. Two single-shot images of fuel injection in air are shown in Figure (9a) and (9b). The images show that the fuel concentration distributions vary considerably from laser shot to laser shot. The images were taken during combustion conditions with experimental conditions corresponding with 10 atm pressure and 675K inlet air. These images show the potential of one-dimensional Raman imaging to simultaneously show the location of oxygen, nitrogen, hydrocarbons, and water, and also, with appropriate calibration, to quantify these concentrations. Spatial distribution of mixture fractions along the imaged laser beam can be obtained by an appropriate "binning" of the CCD, where rows of pixels are added to improve the signal-to-noise ratio. The number of bins determines the spatial resolution.

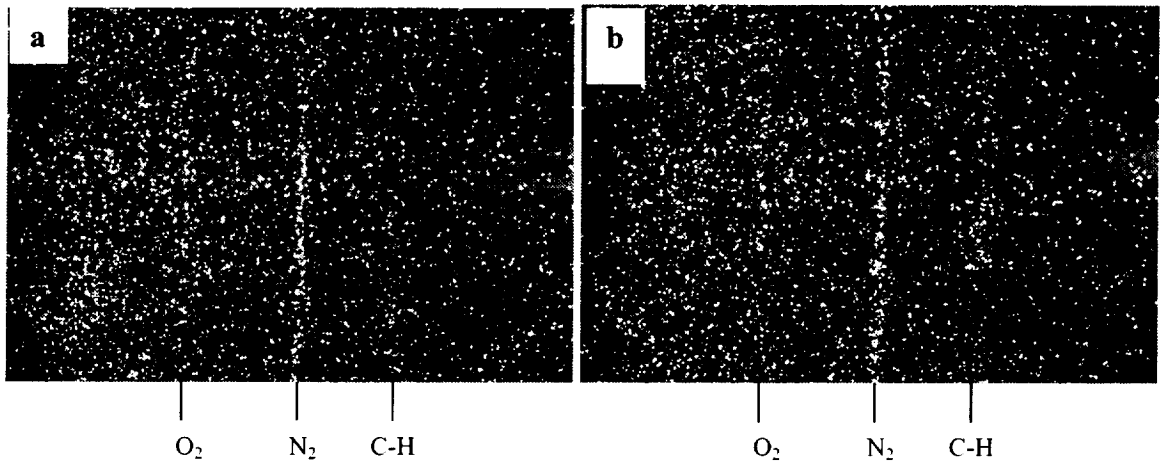

Figure 9: Single-shot images of fuel injection in air, a: some fuel visible in lower part of image; b. fuel visible mostly in center of image.

Figure (10) shows both a single-shot (left) and an averaged spectrum (right) of fuel injected in air at 755K and 10 atm. The ratio of oxygen versus nitrogen peak height is the same as for the pure air, which indicates that no reaction has taken place. The broad peak appearing between 650 and 660 nm in the fuel injection spectrum can not be explained by the presence of water, and instead appears to be caused by OH stretching vibration in alcohols within the liquid fuel.[7] This assumption is supported by the finding that the peak grows and broadens substantially with lower temperatures, where less of the fuel has evaporated. The nitrogen peak ratio between the fuel injection and no-injection cases is approximately 1:10. With a temperature ratio of only 4:9, this indicates that fuel has replaced air in substantial amounts. In a number of spectra, a peak appears between the oxygen and nitrogen lines, corresponding with a Raman shift of 1872 cm^{-1}. This seems to coincide with emission from excited nitrogen plasma[8], which could be caused by the high laser fluence in the probe volume of the beam. Elimination of this peak can be achieved by moving the focal volume out of the imaged section or by reducing the laser pulse energy.

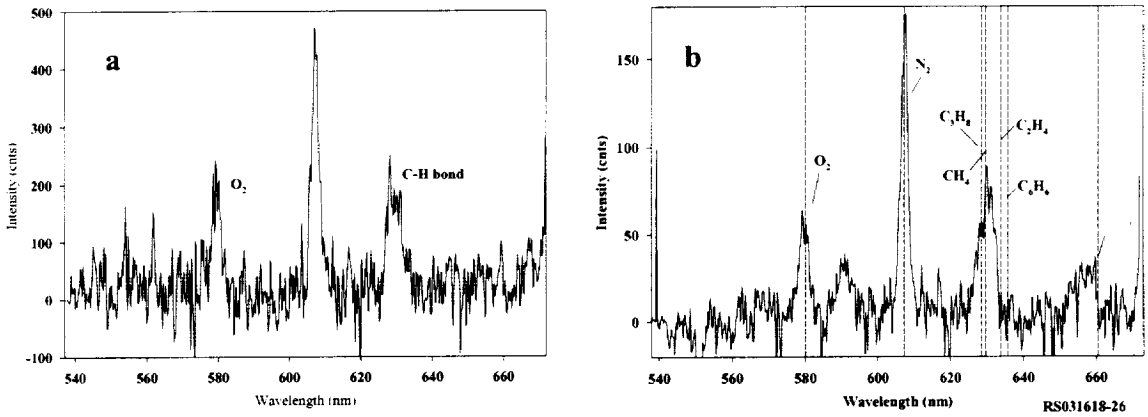

Figure 10: a. Single-shot spectrum, and b. Averaged spectrum of fuel injected in air at 755K and 10 atm.

SUMMARY AND CONCLUSIONS

A review of recent advanced diagnostic measurements made in the engine research facility at NASA Glenn Research Center has been presented. We have shown that with the aid of innovative post-processing computer algorithms, planar imaging techniques such as PMie scattering and PLIF can be successfully employed to generate cross-flow images at a wide range of test conditions in large-scale test rigs. The resulting measurements can be used to parameterize combustor and subcomponent performance at flow conditions expected in novel high pressure combustor concepts. Internal flow structures presented herein are now readily observed at these extreme conditions and clearly demonstrate the ability and sensitivity of these imaging techniques at delineating different flow phenomena and/or species. The fuel to air contour plots, generated from compiled 3-D image blocks, plainly show for the first time ever the fuel distribution across the mixing region of the flow stream. These results have revealed that even a combustor operating at globally lean conditions (f/a = 0.03), produces locally fuel-rich pockets in excess of stoichiometric immediately downstream of the fuel injector exit plane. With recent modifications to the experimental setup, future experiments will better account for laser sheet attenuation and fluorescence quenching in a move to quantify these measurements.

Taking advantage of the increased signal with pressure, we have also presented what we believe to be the first visible1-D Raman images of speciation obtained from a gas turbine combustor burning jet fuel at high pressure conditions. These measurements have demonstrated the feasibility of simultaneously acquiring single-shot spectra and distribution for multiple species. Further improvements to this visible wavelength, 1-D Raman technique could lead to simultaneous temperature and species measurements.

Information such as that presented herein is only possible through nonintrusive laser-induced imaging techniques. These have proven to be invaluable as diagnostic tools, critical to engine and injector designers since only in this manner can the flow fields and various combustion phenomena be directly observed and analyzed in real-time.

REFERENCES

1. V. Lyons and R. Niedzwiecki, "Combustor Technology for Future Small Gas Turbine Aircraft," *NASA Technical Memorandum*, TM-106312, August 1993.

2. R.J. Locke, Y.R. Hicks, R.C. Anderson, K.A. Ockunzzi, and H.J. Shock, "Imaging of Combustion Species in a Radially Staged Gas Turbine Combustor," *CPIA Pub.* 653, Vol. 1, Proceedings of the 33rd JANNAF Combustion Subcommittee and Propulsion Systems Hazards Subcommittee Joint Meeting, Monterey, California, November 1996.

3. R.J. Locke, Y.R. Hicks, R.C. Anderson, and M. Zaller, "Optical Fuel Injector Patternation Measurements in Advanced Liquid-Fueled, High Pressure Gas Turbine Combustors," *Combust. Sci. and Tech.*, Vol. 138, pp. 297-311, 1998.

4. Y.Gu, E.W. Rothe, G.P. Reck, R.C. Anderson, Y.R. Hicks, M. Zaller, Q-V. Nguyen, and R.J. Locke, "1-D, UV-Raman Imaging from a High-Pressure, Jet-A Fueled, Gas Turbine Combustor," AIAA Paper No. 2000-0773, 38th Aerospace Science Meeting and Exhibit, Reno, Nevada, January, 2000.

5. R. Locke, R.C. Anderson, M. Zaller, and Y.R. Hicks, "Challenges to Laser-Based Imaging Techniques in Gas Turbine Combustors Systems for Aerospace Applications," AIAA Paper 98-2778, 20th Advanced Measurement and Ground Testing Technology Conference, Albuquerque, New Mexico, June, 1998.

6. P. C. Miles, "Raman Line Imaging for Spatially and Temporally Resolved Mole Fraction Measurements in Internal Combustion Engines," *Applied Optics*, Vol. 38, No.9, pp. 1714 -1732, 1999.

7. B. Mewes, G. Bauer, and D. Brueggemann "Fuel Vapor Measurements by Linear Raman Spectroscopy Using Spectral Discrimination From Droplet Interferences", *Applied Optics*, Vol. 38, No. 6, p. 20, 1999.

8. C.M. Gittiins, S.U. Shenoy, H.R. Aldag, D.P. Pacheco, M.F. Miller, and M.G. Allen, "Measurements of Major Species in a High Pressure Gas Turbine Combustion Simulator Using Raman Scattering," AIAA Paper 2000-0772, 38th Aerospace Sciences Meeting and Exhibit, Reno, NV, January, 2000.

REPORT DOCUMENTATION PAGE

Form Approved
OMB No. 0704-0188

1. AGENCY USE ONLY (*Leave blank*)	2. REPORT DATE	3. REPORT TYPE AND DATES COVERED
	August 2001	Technical Memorandum

4. TITLE AND SUBTITLE

Non-Intrusive, Laser-Based Imaging of Jet-A Fuel Injection and Combustion Species in High Pressure, Subsonic Flows

5. FUNDING NUMBERS

WU–714–02–40–00

6. AUTHOR(S)

Randy J. Locke, Yolanda R. Hicks, Robert C. Anderson, and Wilhelmus A. de Groot

7. PERFORMING ORGANIZATION NAME(S) AND ADDRESS(ES)

National Aeronautics and Space Administration
John H. Glenn Research Center at Lewis Field
Cleveland, Ohio 44135–3191

8. PERFORMING ORGANIZATION REPORT NUMBER

E–12960

9. SPONSORING/MONITORING AGENCY NAME(S) AND ADDRESS(ES)

National Aeronautics and Space Administration
Washington, DC 20546–0001

10. SPONSORING/MONITORING AGENCY REPORT NUMBER

NASA TM—2001-211113

11. SUPPLEMENTARY NOTES

Prepared for the Joint First Modeling and Simulation Subcommittee Meeting, 25th Airbreathing Propulsion Subcommittee Meeting, 37th Combustion Subcommittee Meeting, and the 19th Propulsion Systems Hazards Subcommittee Meeting sponsored by the Joint Army-Navy-NASA-Air Force, Monterey, California, November 13–17, 2000. Randy J. Locke and Wilhelmus A. de Groot, QSS Group, Inc., 2000 Aerospace Parkway, Brook Park, Ohio 44142; and Yolanda R. Hicks and Robert C. Anderson, NASA Glenn Research Center. Responsible person, Yolanda R. Hicks, organization code 5830, 216–433–3410.

12a. DISTRIBUTION/AVAILABILITY STATEMENT

Unclassified - Unlimited
Subject Category: 35 Distribution: Nonstandard

Available electronically at http://gltrs.grc.nasa.gov/GLTRS

This publication is available from the NASA Center for AeroSpace Information, 301–621–0390.

12b. DISTRIBUTION CODE

13. ABSTRACT ***(Maximum 200 words)***

The emphasis of combustion research efforts at NASA Glenn Research Center (GRC) is on collaborating with industry to design and test gas-turbine combustors and subcomponents for both sub- and supersonic applications. These next-generation aircraft combustors are required to meet strict international environmental restrictions limiting emissions. To meet these goals, innovative combustor concepts require operation at temperatures and pressures far exceeding those of current designs. New and innovative diagnostic tools are necessary to characterize these flow streams since existing methods are inadequate. The combustion diagnostics team at GRC has implemented a suite of highly sensitive, nonintrusive optical imaging methods to diagnose the flowfields of these new engine concepts. By using optically accessible combustors and flametubes, imaging of fuel and intermediate combustion species via planar laser-induced fluorescence (PLIF) at realistic pressures are now possible. Direct imaging of the fuel injection process through both planar Mie scattering and PLIF methods is also performed. Additionally, a novel combination of planar fuel fluorescence imaging and computational analysis allows a 3-D examination of the flowfield, resulting in spatially and temporally resolved fuel/air volume distribution maps. These maps provide detailed insight into the fuel injection process at actual conditions, thereby greatly enhancing the evaluation of fuel injector performance and other combustion phenomena. Stable species such as CO_2, O_2, N_2, H_2O, and hydrocarbons are also investigated by a newly demonstrated 1-D, spontaneous Raman spectroscopic method. This visible wavelength Raman technique allows the acquisition of quantitative, stable species concentration measurements from the flow.

14. SUBJECT TERMS	15. NUMBER OF PAGES
Subsonic combustion; Liquid fuel; Imaging; Optical diagnostics	17
	16. PRICE CODE

17. SECURITY CLASSIFICATION OF REPORT	18. SECURITY CLASSIFICATION OF THIS PAGE	19. SECURITY CLASSIFICATION OF ABSTRACT	20. LIMITATION OF ABSTRACT
Unclassified	Unclassified	Unclassified	